

# Photonic crystal fibers formed by air channels with a corrugated boundary

A V Shilov<sup>1</sup>, S S Miheev<sup>1</sup>, A B Sotsky<sup>1</sup>, M M Nazarov<sup>2</sup>, L I Sotskaya<sup>3</sup>,  
K A Bzheumikhov<sup>4</sup> and Z Ch Margushev<sup>4</sup>

<sup>1</sup>Mogilev State University, Kosmonavtov street 1, Mogilev, Republic of Belarus, 212022

<sup>2</sup>Kurchatov Institute National Research Center, Akademika Kurchatova pl. 1, Moscow, Russia, 123182

<sup>3</sup>Belarusian-Russian University, Prospect Mira 43, Mogilev, Republic of Belarus, 212024

<sup>4</sup>Institute of Computer Science and Problems of Regional Management of the Kabardino-Balkarian Scientific Center of the RAS, Armand street 37a, Nalchik, KBR, Russia, 360000

e-mail: undersv@yandex.ru

**Abstract.** We analyzed problem of optimization of the configuration of photonic-crystal fibers with a hollow core for transmission of broad band terahertz pulses. With the use of local modes of a dielectric corrugated surface, we shown that minimization of the attenuation and dispersion of the group velocity of the terahertz radiation can be achieved by using air channels with a corrugated boundary.

## 1. Introduction

The interest in terahertz (THz) radiation is now increased significantly, since this range turned out to be promising for a number of applications in security and medical systems. Manufacturing of fibers for the THz radiation transporting is complicated by the fact that this radiation is strongly absorbed by all known materials. Therefore, the most promising THz fibers are ones that transmit the THz signal through the fiber hollow core [1]. Among such fibers metal-dielectric capillaries demonstrate the record low ( $\sim 1$  dB / m) modal attenuation [2 - 5]. However, these fibers are difficult in manufacturing. Besides they usually work in multimode regime that makes difficult their use in THz spectroscopy and sensing. Competitive alternative to metal-dielectric capillaries is hollow core dielectric fibers [1]. The simplest of these fibers is a capillary tube with smooth walls [6, 7]. The disadvantage of this fiber is the significant influence of the environment on the THz field transmitted through its core. This drawback can be eliminated by introducing a photonic crystal structure in the fiber cladding that isolates radiation transmitted along the hollow fiber core from the environment due to the Bragg reflection [1].

This paper presents results of theoretical and experimental investigations of photonic crystal fibers formed by circular capillary systems surrounding a hollow core and photonic crystal fibers with a hollow core of a corrugated cross section. Calculations of modal characteristics of the fibers are performed by the method of Green's functions in which local cladding modes are used [8]. This



accurate frequency domain mode solver found both the fields and dispersion characteristics of modes and no use any artificial screens for account for the mode leakage.

## 2. Description of the method

Cross-sections of the capillary fibers under investigation and computed fields of their fundamental modes are shown in figure 1. Here and below polypropylene is considered as the fiber material. Its dielectric constant, measured us with the time-domain terahertz spectroscopy (TDS) method, is  $\varepsilon = 2.247 - i0.0036$ . This value is almost constant in the frequency range from 0.1 to 3THz. The optical mode density (light spots in the central region of figures 1 a-c) is the normalized to its maximum z-component of the mode Poynting vector. The angular diagrams of the mode field radiation (multi petal structures) are normalized to their maxima transverse components of the Poynting vector computed on the outer perimeter of the fiber cross-section.

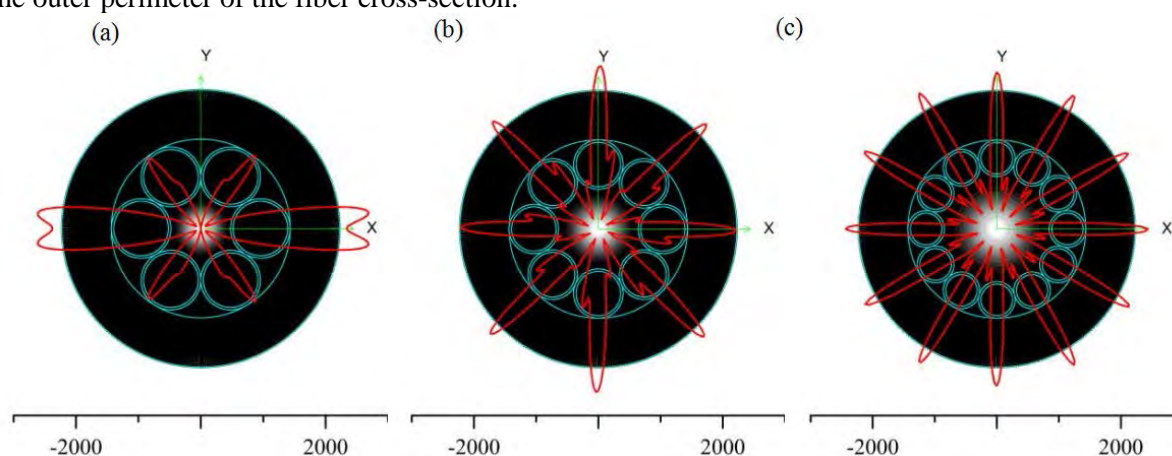


**Figure 1.** Optical densities (white half tones) and angular radiation diagrams (red curves) of the fields at the frequency of 2.1 THz of the fundamental modes of THz photonic crystal fibers with a hollow core and a cladding formed by circular systems of various numbers of polypropylene capillaries (a – 6 capillaries, b – 8 capillaries, c – 12 capillaries) with a wall thickness  $d=40.7 \mu\text{m}$ . The space scales are in  $\mu\text{m}$ .

Experimental data for the temporal and frequency characteristics of THz pulses at the input and output ends of an eight-capillary fiber are shown in figure 2. The outer diameter of this fiber, as in figure 1, is 4.5 mm. However, due to technological limitations, the thickness  $d$  of the capillary walls significantly exceeds the optimal value considered above and is equal to  $170 \mu\text{m}$ .

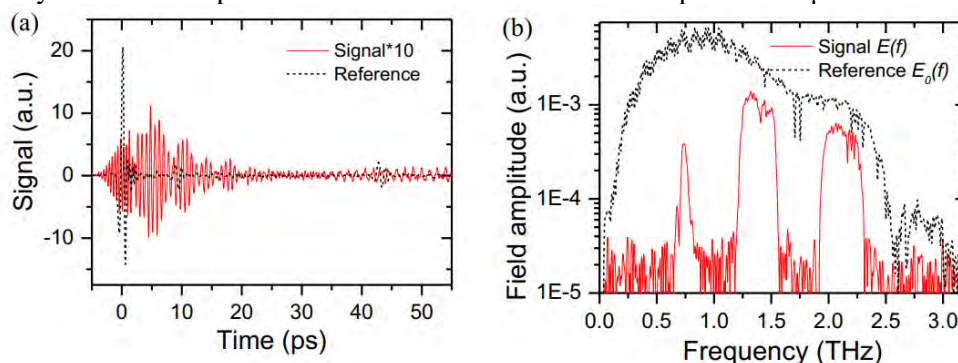


**Figure 2.** Measured parameters of the THz pulse (temporal (a) and frequency (b) domaine). Dashed and solid curves correspond to a pulse at the input and output ends of the 20 cm eight-capillary fiber.

Theoretical and experimental results for the dispersion characteristics of the given fiber are presented in figure 3. Here  $\beta$  is the dimensionless mode propagation constant.

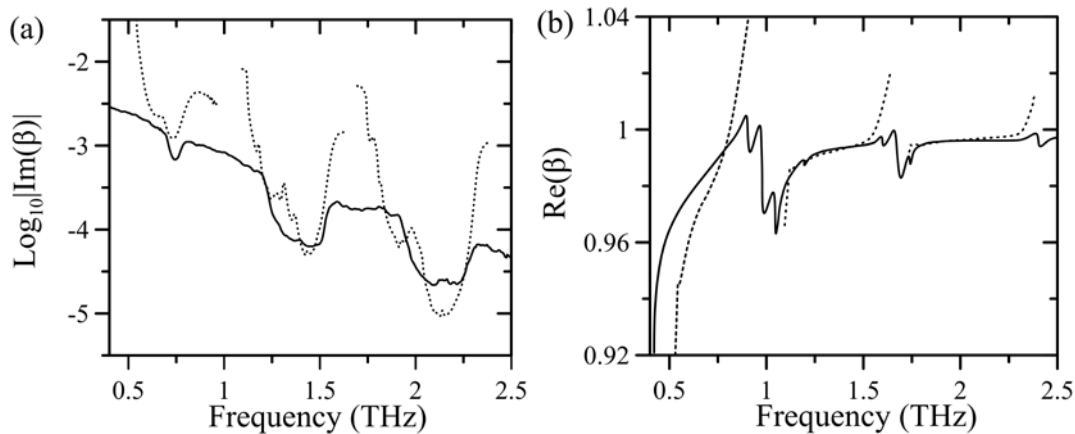


**Figure 3.** Theoretical (dashed curves) and experimental (solid curves) dispersion dependencies for the fundamental mode of the eight-capillary fiber.

According to figure 3, theory and experiment are in fairly good agreement, which indicates the single-mode regime of fiber action. At the same time, the attenuation of the fundamental mode of the fiber is rather large (its minimum in the third transparency window at a frequency of 2.15 THz is 7.1 dB/m).

Qualitative reasons for the fiber structure optimization from the point of view of minimization of the transmitted THz signal attenuation follow from figure 1.

Presented in the figure 1 radiation diagrams indicate that the radiation leak from the hollow core of the fiber by rays passing through the centres of the capillaries, encountering in path almost plane interfaces and practically does not leak through narrow areas in the vicinity of points of contact between neighbouring capillaries. This suggests reducing the "weight" of areas with plane-parallel for meridional rays interfaces in the fiber cross-section. Cladding with corrugated cross-section allows to perform this reduce. Cross-sections of the corresponding fibers are shown in figure 4. Outside the polypropylene cladding is air. The thickness of the cladding in the plane-parallel regions of the corrugate is chosen from the relation

$$d \lambda^{-1} = (0.5k + 0.25)(\varepsilon - 1)^{-0.5} \quad (k = 0, 1, \dots), \quad (1)$$

where  $\lambda$  is a wavelength, that provides interference minima of reflectivity for sliding rays forming the mode field [9]. In calculations we used the value of  $d = 67.65 \mu\text{m}$ , related to  $k = 0$  in (1) at  $\lambda = 300 \mu\text{m}$ .

Figures 4b and 4d show fragments of the optical density of the fundamental  $H_x$  modes in the vicinity of claddings of the fibers presented in figures 4a and 4b, respectively. The maxima of the densities in the cladding material are observed in the vicinity of the edges facing to the hollow core of the fibers. The decrease of these maxima and the material absorption of the mode energy can be achieved by optimizing the form of the corrugation.

Dispersion characteristics of corrugated fibers are presented in figures 5 and 6.

According to figure 5, at certain frequency intervals, the attenuation of the modes of the proposed fibers is lower than the attenuation of the mode of the capillary tube with the same outer diameter (3 mm). This effect is especially expressed for fiber with 16 periods (see figure 5b). For example, for the frequency 1.1 THz the calculated attenuation of the fundamental mode of this fiber is equal to 1.3 dB/m that is in several times smaller than the attenuation of the fundamental mode of the polypropylene capillary tube (8 dB/m). At the same time the corrugation of the cladding complicates the dispersion characteristics of the modes in comparison with the analogous characteristics for the capillary tube with smooth walls.

It is interesting to note that in figure 5 regions of the anomalous dispersion of the real part of the mode propagation constants are matched with maxima of the mode attenuation. This effect of anomalous dispersion is diffractive in nature, and it is similar to the usual effect of anomalous

dispersion having an electronic nature. The effect can be used in the maximization of sensitivity of THz sensors. Note also a low dispersion of the group velocity of the modes in frequency intervals corresponding to minima of the  $|\text{Im}\beta|$  frequency dependencies (see figure 6).

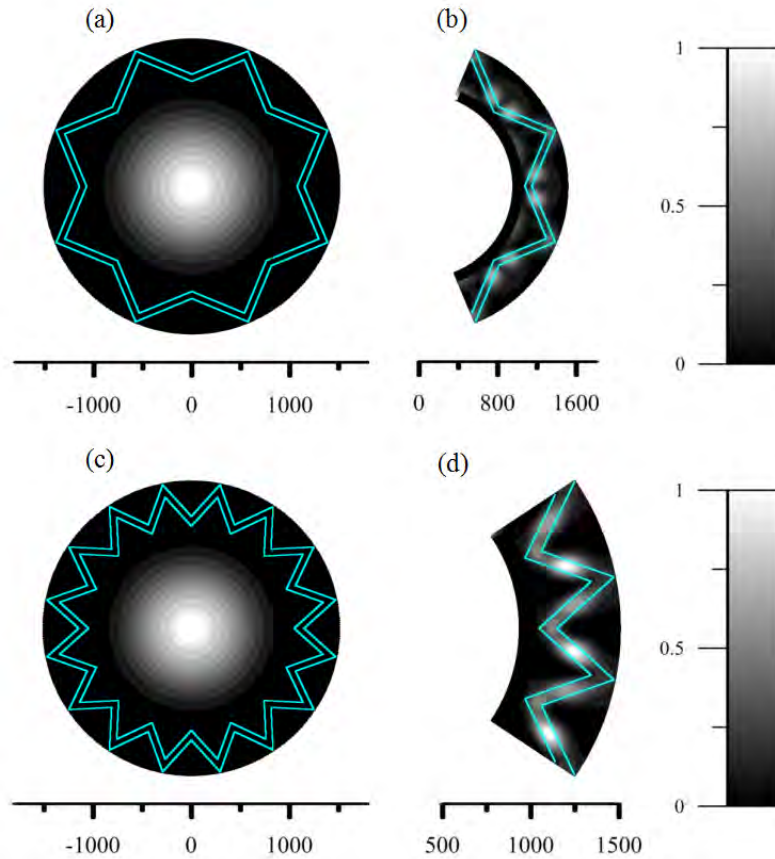


**Figure 4.** Optical densities of the fundamental mode of hollow photonic crystal fibers with a corrugated cladding containing 8 (a, b) and 16 (c, d) periods at the frequency of 1.12 THz.

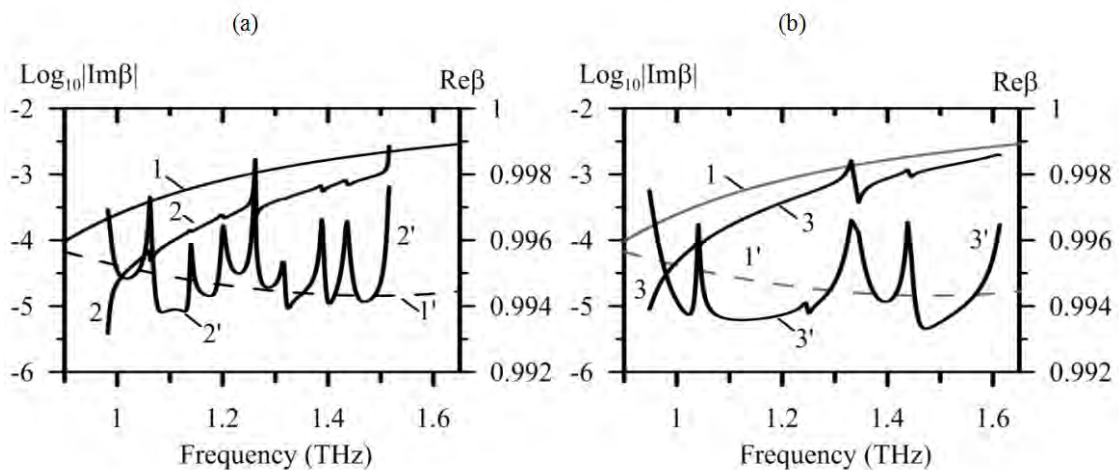


**Figure 5.** Dispersion dependencies of the fundamental modes of a capillary tube with smooth walls (1, 1') and hollow core photonic crystal fibers with a corrugated cladding containing 8 (2, 2') and 16 (3, 3') periods. Curves 1, 2, 3 refer to the real part, 1', 2', 3' – to the imaginary part of the mode propagation constants.

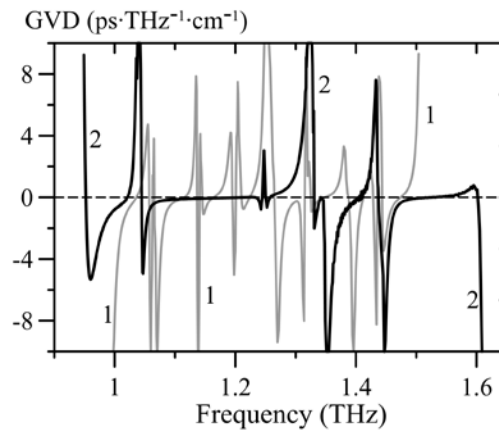


**Figure 6.** Group velocity dispersion of the fundamental modes of hollow photonic crystal fibers with the corrugated cladding containing 8 (curve 1) and 16 (curve 2) periods.

In accordance with figure 5, at certain frequency intervals the attenuation of the modes of corrugated fibers is lower than the attenuation of the mode of the capillary tube with the same outer diameter (3 mm).

Now we are developing the technology of manufacturing corrugated polypropylene THz fibers. Figure 7 shows a photograph of the sections of the samples previously obtained in this way.

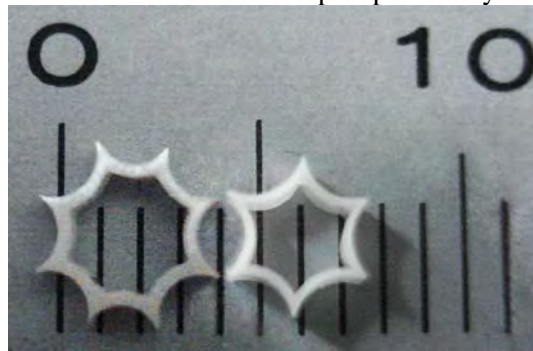


**Figure 7.** Cross sections of experimental samples of polypropylene THz fibers with a corrugated cladding. The scale division is 1mm.

It should be noted, that the configuration of the experimental fiber samples differs from the configurations discussed above due to the current technological limitations. The inner perimeter of the cross section of the fibers in figure 7 consists of  $N$  segments of circles of the radius  $\rho$  (in figure 7 two cases of  $N=8$  and  $N=6$  are presented). The value of  $\rho$  satisfies the inequality

$$\rho \leq [d + R \sin(\pi N^{-1})][1 - \sin(\pi N^{-1})]^{-1}, \quad (2)$$

where  $d$  is the polypropylene wall thickness,  $R$  is the radius of the fiber hollow core (it is the minimal distance from the fiber centre to the inner perimeter of its cross section). The distance from the fiber centre to the farthest points of its perimeter is

$$r_g = (R + \rho) \cos(\pi N^{-1}) - \left\{ [(R + \rho) \cos(\pi N^{-1})]^2 - (R + d)(R + 2\rho - d) \right\}^{0.5}. \quad (3)$$

In the case of capillary fibers (figure 1) the same distance is

$$r_c = R[1 + \sin(\pi N^{-1})][1 - \sin(\pi N^{-1})]^{-1}. \quad (4)$$

At the condition  $R \gg d$  that provides a low THz signal attenuation [10] it follows from Eqs (2) – (4), that

$$r_g r_c^{-1} \leq \cos(\pi N^{-1})[1 + \sin(\pi N^{-1})]^{-1}. \quad (5)$$

Since transmitting properties of the fiber are determined mainly by the radius of the fiber's hollow core and segments of the capillaries adjacent to the hollow core, it follows from (5) that the transition from the capillary to the corrugated structure of the fiber allows to considerably reduce its diameter without sacrificing the transmitting properties. For example, at  $N=6$   $r_g r_c^{-1} \leq 0.67$  and at  $N=5$   $r_g r_c^{-1} \leq 0.63$ .

Modal properties of fibers with the described configuration are illustrated in figure 8, which refers to the fundamental  $H_x$  mode. Here, the mode irradiation diagram represents the angular dependence of the transverse component of the Poynting vector on the circle of the radius  $r_g$ , normalized to the maximum of the longitudinal (directed along the fiber axis) component of the Poynting vector.

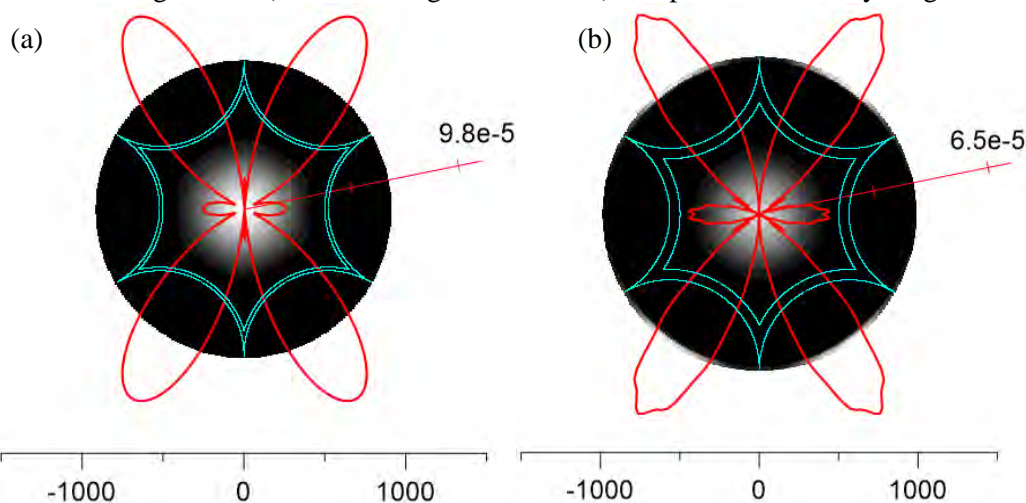


**Figure 8.** Optical densities and irradiation diagrams of the fundamental  $H_x$  mode of fibers with corrugated cross sections at  $\lambda = 96.8 \mu\text{m}$  (wavelength of a quantum-cascade laser irradiation),  $d = 22 \mu\text{m}$  ( $k = 0$  in (1)) (a) and  $d = 65 \mu\text{m}$  ( $k = 1$  in (1)) (b). Calculations are made at  $R = 500 \mu\text{m}$  and the values of  $\rho$  computed from (2) where sign of equality is used.

Figure 8a corresponds to the dimensionless mode propagation constant  $\beta = 0.997567 - i8.8 \cdot 10^{-6}$ . In this case the contribution of the confinement losses to the imaginary part of  $\beta$ , computed through the ratio of the transverse and longitudinal energy flows of the mode [8], is  $\text{Im}\beta_l = -7.5 \cdot 10^{-6}$ . Figure 8b corresponds to  $\beta = 0.997542 - i1.0 \cdot 10^{-5}$  and  $\text{Im}\beta_l = -5.3 \cdot 10^{-6}$ . From a comparison of these values it is evident that an increase in the thickness of the polypropylene wall reduces the mode confinement losses, however it leads to an increase in the mode attenuation due to an increase of the overlap region between the mode field and the absorbing material.

We measured by the TDS method the spectrum of THz irradiation attenuation in a fabricated sample of a polypropylene THz fiber of 25 cm length. Both the microscopic photo of this sample cross section and a comparison of theoretical and experimental attenuation spectra are presented in figure 9. The theoretical data are obtained with account for the fiber fundamental mode only.

### 3. Conclusion

Some discrepancy between the theory and experiment in Fig. 9b can be explained by the presence of higher order modes at the output end of the fiber due to its relatively small length and by imperfections of the polypropylene walls. In particular, polypropylene wall thickness variations reached 30%. The last drawback will be eliminated by improving the technology of manufacturing the fibers.



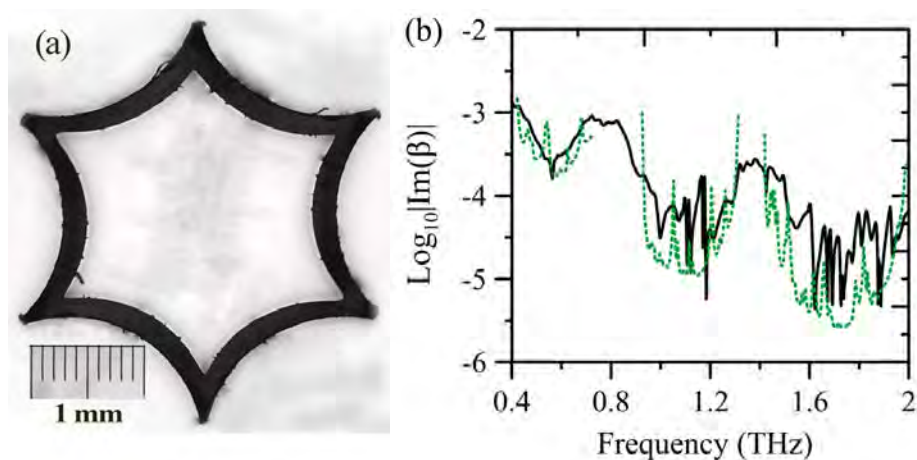


**Figure 9.** Microscopic photo of cross-section of an experimental waveguide sample investigated with the TDS method (a) and a comparison of the experimental irradiation attenuation with the computed attenuation of the sample's fundamental mode (b); solid curve refers to the experiment, dashed curves – the theory.

#### 4. References

- [1] Atakaramians Sh, Afshar Sh V, Monro T M and Abbott D 2013 *Advances in Optics and Photonics* **5** 69
- [2] Harrington J A, George R and Pedersen P 2004 *Optics Express* **12** 5263
- [3] Matsuura Y and Takeda E 2008 *Journal of the Optical Society of America B* **25** 1949
- [4] Ito K, Katagiri T and Matsuura Y 2017 *Journal of the Optical Society of America B* **34** 60
- [5] Sotsky A B, Shilov A V and Sotskaya L I 2017 Propagation of terahertz pulses in capillary waveguides with a metalized cladding *Computer Optics* **41** 803 DOI: 10.18287/2412-6179-2017-41-6-803-811
- [6] Daru C 2010 *Journal of Lightwave Technology* **28** 2708
- [7] Hualong B, Nielsen K, Bang O and Jepsen P 2015 *Scientific Reports* **5** 76201
- [8] Sotsky A B 2011 *Theory of optical waveguide elements* (Mogilev: A A Kuleshov State University Press) pp 151-166
- [9] Nazarov M M, Kitai M S, Sokolov V I, Bzheumihov K A, Margushev Z Ch, Sotsky A B, Shilov A V, Sotskaya L I, Goncharenko A M and Sinitsyn G V 2016 *Journal of Applied Spectroscopy* **83** 565
- [10] Nazarov M M, Shilov A V, Bzheumihov K A, Margushev Z Ch, Sokolov V I, Sotsky A B and Shcurinov A P 2018 *IEEE Transactions on Terahertz Science and Technology* **8** 183

#### Acknowledgments

These studies were done as part of the task 1.3.03, "Development of a Theory for Optical Monitoring Methods for Nanosized Thin-Film Structures," of the State program for scientific research "Photonics, Opto- and Microelectronics", were supported by the Belarusian Republican Foundation for Fundamental Research (grant No. F18R-143) and the Russian Foundation for Basic Research (grant No. 18-52-16024, 18-52-00040).